

# Photoquenching Parameters for Commonly Used Laser Dyes

S. Speiser\* and N. Shakkour

Department of Chemistry, Technion-Israel Institute of Technology, Haifa 32000, Israel

Received 23 March 1985/Accepted 3 June 1985

**Abstract.** Laser dyes which are commonly used in pulsed laser pumped dye laser (PLPDL) systems have been investigated. It is shown that photoquenching plays an important role in the pumping process of all laser dyes, determining the efficiency of the PLPDL. Molecular parameters, such as absorption cross sections at various pumping wavelengths and fluorescence lifetimes of the  $S_n(n > 1)$  excited electronic states of laser dyes, have been determined utilizing the photoquenching technique.

**PACS:** 35, 42.55, 42.60

The absorption properties of molecular systems are changed when subjected to high-intensity lasers. At very high intensities stimulated emission from an unrelaxed excited singlet vibronic state ( $S_1$ ) competes with the pumping of this level. As a result optical bleaching occurs, which is manifested in a violation of the Beer-Lambert absorption law. This effect is widely used in Q-switching and mode locking of lasers by saturable absorbers [1]. At moderate laser powers stimulated emission rate is too small to compete with vibrational relaxation rate,  $k_{vib}$ , of  $S_1$ . However, pumping of  $S_1$  to high-lying singlet states  $S_n(n \geq 2)$  will compete with its fluorescence decay (Fig. 1). Consequently, photoquenching of the fluorescent level occurs. This is manifested in a unique intensity dependent fluorescence yield  $Y(S_1)$  per molecule and intensity dependent quantum yield  $\phi = Y(S_1)/[\sigma_{01}f + \sigma_{1n}(1-f)]I_P \Delta t$ , where  $\sigma_{01}$  is the absorption cross section for the  $S_0 \rightarrow S_1$  transition,  $I_P$  is the laser pump intensity,  $f$  is the fraction of molecules at  $S_0$  and  $\Delta t$  the laser pulse duration [2]. For large molecules whose typical fluorescence life times are about 1 ns, a steady state is reached even at ns pulse excitation. For optically thin samples  $Y(S_1)$  is given by [2].

$$Y(S_1) = (\phi_0 + \tau_{10}\phi_{n1}\sigma_{1n}I_P)\sigma_{01}I_P \Delta t / (1 + \tau_{10}\sigma_{01}I_P + \tau_{10}\tau_{n1}\sigma_{01}\sigma_{1n}I_P^2), \quad (1)$$

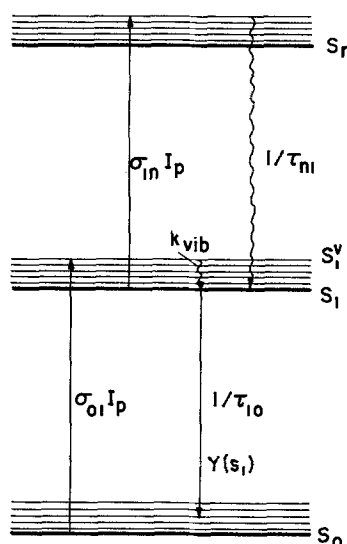


Fig. 1. Schematic level diagram for laser dye pumped by an intense laser, showing the radiative ( $\rightarrow$ ) and non-radiative ( $\rightsquigarrow$ ) transitions and the photophysical parameters involved in photoquenching of the dye fluorescence

where  $\phi_0$  is the intensity independent quantum yield reached at  $I_P \rightarrow 0$ ,  $\sigma_{1n}$  is the absorption cross section for the  $S_1 \rightarrow S_n$  transition and  $\tau_{n1}$  is the  $S_n$  level lifetime,  $\phi_{n1}$  is the quantum yield of the weak  $S_n \rightarrow S_1$  fluorescence.

In (1) two factors, bleaching and photoquenching, contribute to the nonlinear dependence of  $Y(S_1)$  on  $I_P$ .

\* To whom correspondence should be addressed

When photoquenching is not important  $\sigma_{1n}=0$  and  $Y(S_1)$  saturates at high  $I_p(S) = (\sigma_{01}\tau_{10})^{-1}$ . When this occurs, the transmission  $T$  rises from its low-intensity value. However, for large  $\sigma_{1n}$  the situation is different and one expects  $T$  to decrease at higher  $I_p$ .

It is obvious that studies of intensity-dependent fluorescence intensities and quantum yields are likely to yield significant information about excited-states parameters even under steady-state conditions. This has been demonstrated in many cases [3–15]. In addition, it was shown that photoquenching plays a crucial role in determining the gain and performance of pulsed laser-pumped dye lasers (PLPDL) systems [4–8].

In the present paper we are concerned with laser dyes which are commonly used in PLPDL's. These have been studied by employing photoquenching methods. We demonstrate the ease in obtaining molecular parameters such as  $\tau_{n1}$  and  $\sigma_{1n}$  by the photoquenching technique, which otherwise require fast flash-spectroscopy methods and ps excitation. These parameters can be used for determination of the optimum pumping conditions for a given PLPDL system [4, 6].

## Experimental

A Nd-YAG laser (Quanta-ray DCR-1) operating at the second harmonic (532 nm), at the third harmonic (355 nm), and at the fourth harmonic (266 nm) was

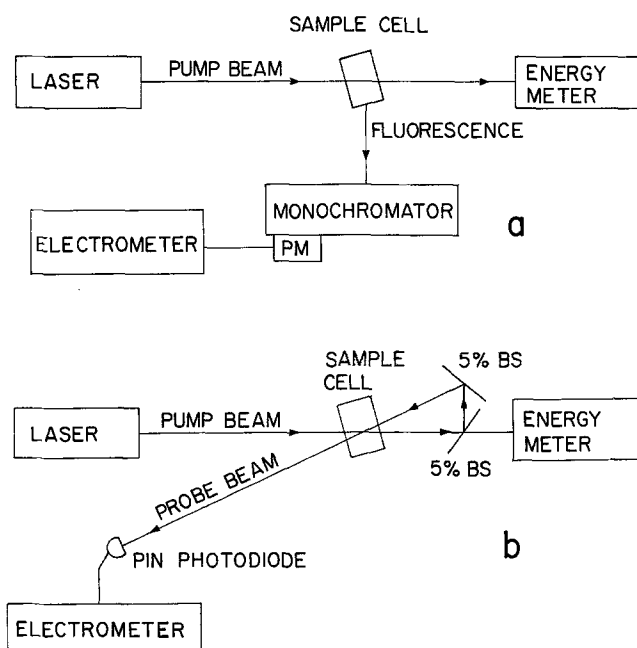


Fig. 2a and b. Experimental set up for photoquenching studies (a) Intensity-dependent fluorescence (b) Intensity-dependent transmission

employed. Laser-energy output was measured using an Ophir Optics 20AQ/20A power meter. Laser-grade dyes (Exciton and Eastman Kodak) dissolved in spectrograde solvents ethanol most dyes, *p*-dioxane for POPOP, bis MSB, DPS, and PDBO) were used. Concentrations were kept at a level which ensured optically thin conditions (O.D.=0.04) for the pump beam. Fluorescence light was collected onto the slit of a Durham 0.5 m monochromator equipment with 1 P28 or Hamamatsu R-777 photomultiplier connected to a Victoreen VTE 1 electrometer. The  $1 \times 1 \text{ cm}^2$  cell was tilted in order to avoid feedback from the walls (Fig. 2a). In some control experiments the transmission  $T$  of the pumped dye was probed by split off  $2.5 \times 10^{-3}\%$  of the pump beam (Fig. 2b).

## Results and Discussion

Typical examples of  $Y(S_1)$  vs.  $I_p$  plots obtained for the laser dyes employed in this study are shown in Figs. 3–8. The same features, a nonlinear  $I_p$  dependence reaching a maximum in  $Y(S_1)$  at some pumping laser intensity  $I_p(\text{max})$ , are typical of photoquenching [7]. All  $Y(S_1)$  vs.  $I_p$  plots were analysed using the photoquenching relation equation (1) [2, 4]. For optically thin samples and for  $I_p < I_p(\text{max})$  the following expression is obtained for the laser-dye fluorescence quantum yield  $\phi$  [2].

$$\phi_0/\phi = 1 + \tau_{10}\sigma_{1n}I_p. \quad (2)$$

Typical photoquenching plots at all pumping wavelengths are shown in Figs. 9–14 for the laser dyes of Figs. 3–8. The fit of these plots to (2), together with the known values of  $\tau_{10}$ , is used to obtain  $\sigma_{1n}$ , a parameter determining the photoquenching properties of the dye. These values are summarized in Table 1.

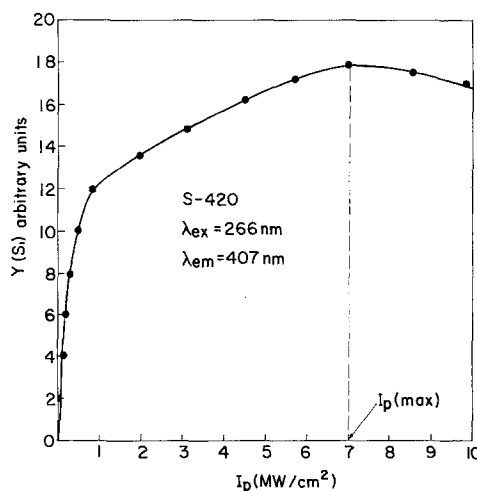


Fig. 3. Typical photoquenching curve,  $Y(S_1)$  vs.  $I_p$ , for the Stilbene-420 laser dye excited at 266 nm

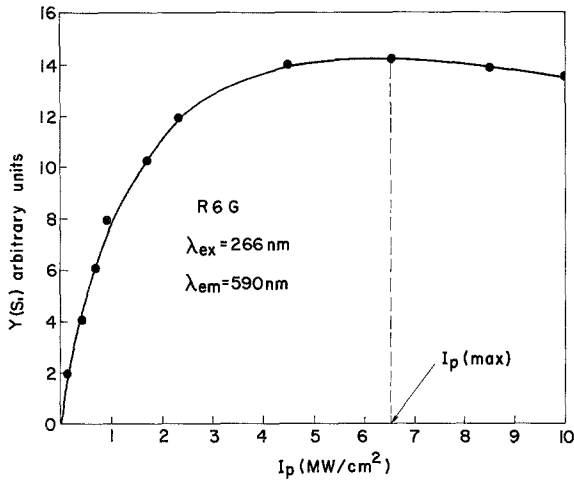


Fig. 4. Typical photoquenching curve,  $Y(S_1)$  vs.  $I_p$ , for the Rhodamine-6G laser dye excited at 266 nm

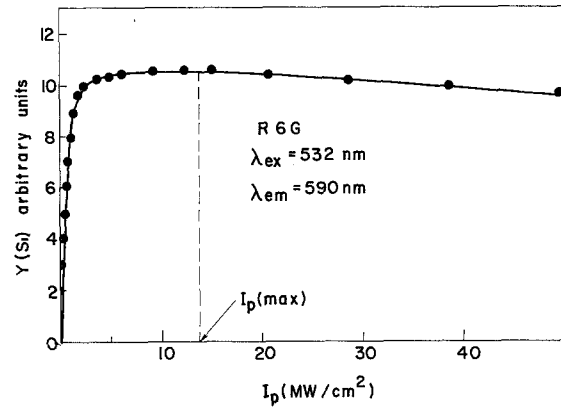


Fig. 7. Typical photoquenching curve,  $Y(S_1)$  vs.  $I_p$ , for the Rhodamine-6G laser dye excited at 532 nm

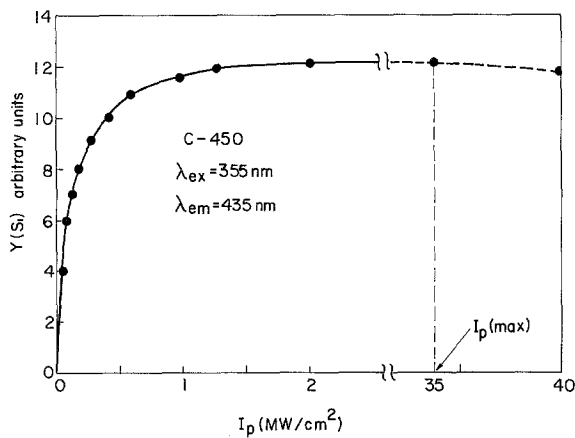


Fig. 5. Typical photoquenching curve,  $Y(S_1)$  vs.  $I_p$ , for the Coumarin-450 laser dye excited at 355 nm

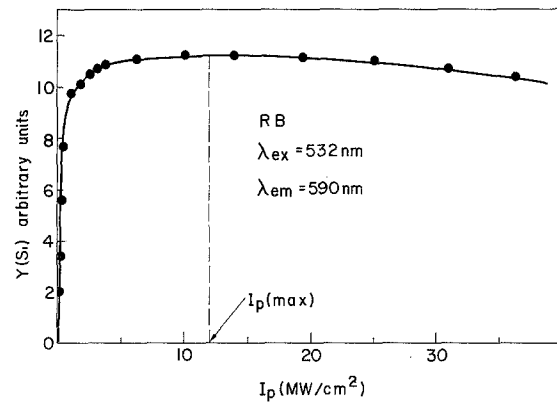


Fig. 8. Typical photoquenching curve,  $Y(S_1)$  vs.  $I_p$ , for the Rhodamine-B laser dye excited at 532 nm

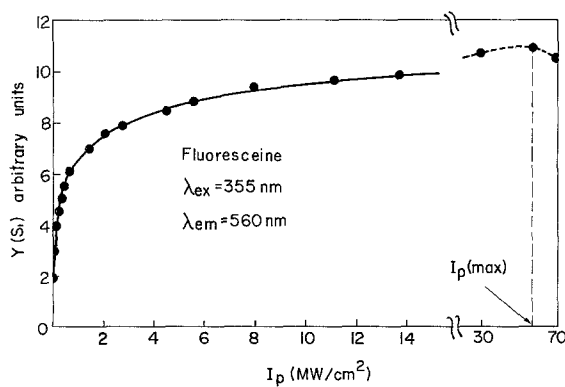


Fig. 6. Typical photoquenching curve,  $Y(S_1)$  vs.  $I_p$ , for the Dichlorofluoresceine laser dye excited at 355 nm

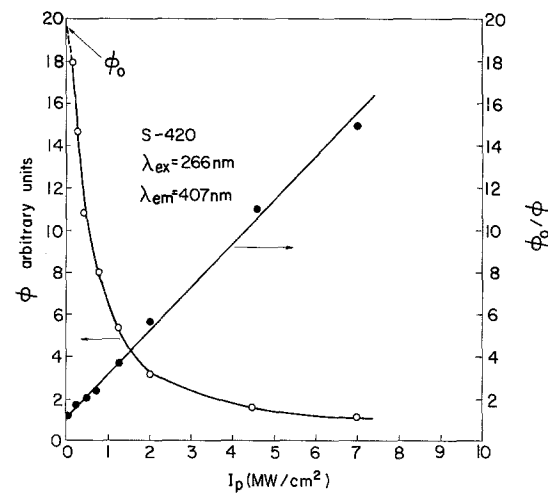


Fig. 9. Photoquenching plots,  $\phi$  vs.  $I_p$  and  $\phi_0/\phi$  vs.  $I_p$ , for the Stilbene-420 laser dye excited at 266 nm (Fig. 2)

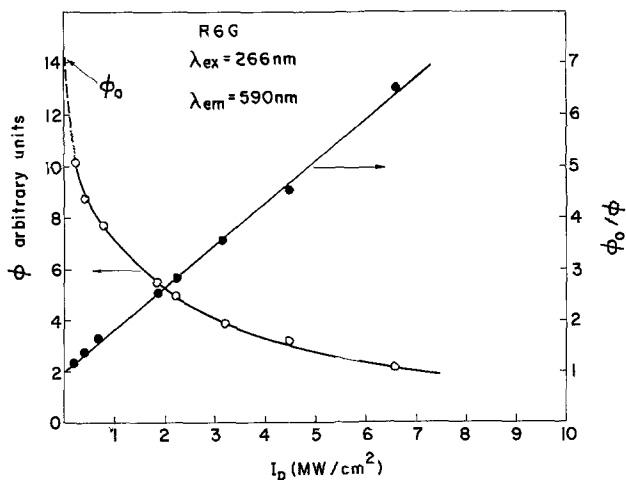


Fig. 10. Photoquenching plots,  $\phi$  vs.  $I_p$  and  $\phi_0/\phi$  vs.  $I_p$ , for the Rhodamine-6G laser dye excited at 266 nm (Fig. 3)

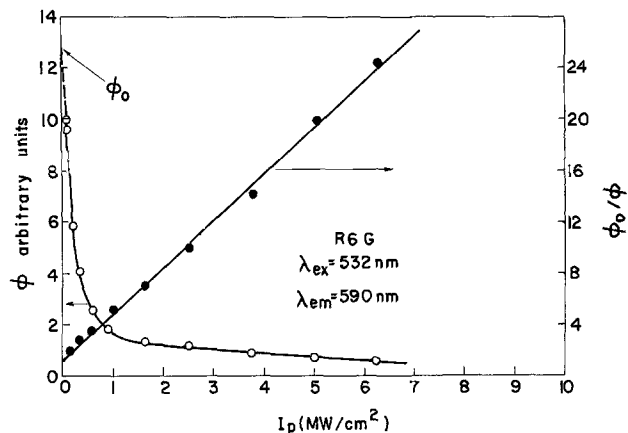


Fig. 13. Photoquenching plots,  $\phi$  vs.  $I_p$  and  $\phi_0/\phi$  vs.  $I_p$ , for the Rhodamine-6G laser dye excited at 532 nm (Fig. 6)

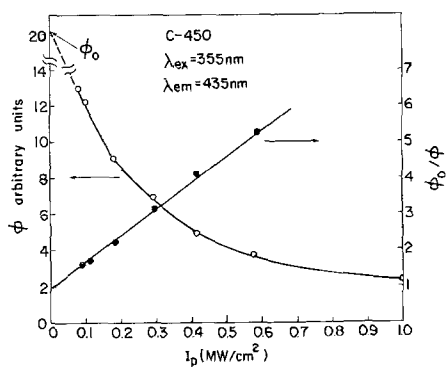


Fig. 11. Photoquenching plots,  $\phi$  vs.  $I_p$  and  $\phi_0/\phi$  vs.  $I_p$ , for the Coumarin 450 laser dye excited at 355 nm (Fig. 4)

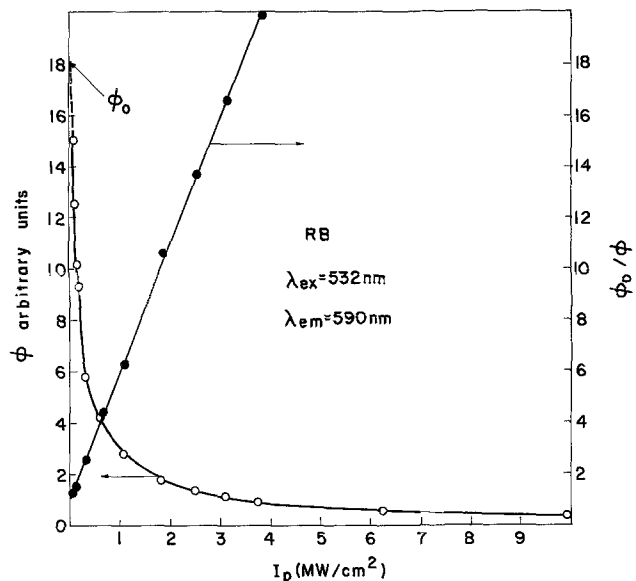


Fig. 14. Photoquenching plots,  $\phi$  vs.  $I_p$  and  $\phi_0/\phi$  vs.  $I_p$ , for the Rhodamine-B laser dye excited at 532 nm (Fig. 7)

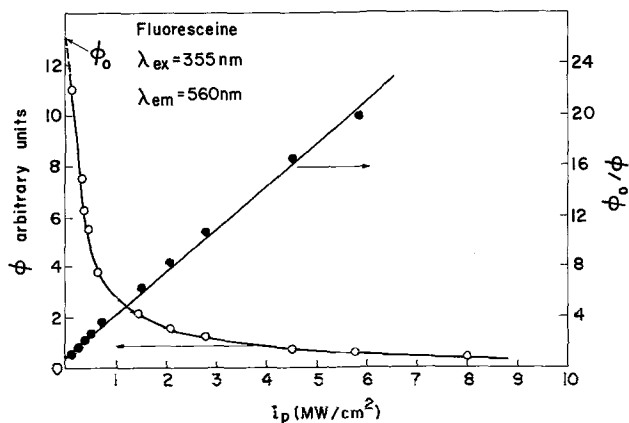


Fig. 12. Photoquenching plots,  $\phi$  vs.  $I_p$  and  $\phi_0/\phi$  vs.  $I_p$ , for the Dichlorofluoresceine laser dye excited at 355 nm (Fig. 5)

An expression for  $I_p(\max)$  can be derived from (1) to read (for low  $\phi_{n1}$ )

$$I_p(\max) = (\sigma_{01}\sigma_{1n}\tau_{10}\tau_{n1})^{-1/2} \quad (3)$$

At the laser intensity range employed a maximum for  $Y(S_1)$  was reached for most of the dyes and the corresponding  $I_p(\max)$  values could be determined. Using the  $\sigma_{1n}$  value obtained from the photoquenching plots, Figs. 9-14 and (2), the  $S_n$  lifetime  $\tau_{n1}$  can be obtained using (3). The results for the photoquenching parameters  $\sigma_{1n}$ ,  $I_p(\max)$ , and  $\tau_{n1}$  at all pumping wavelengths, together with  $\tau_{10}$  literature values

Table 1. Photoquenching parameters  $\sigma_{1n}$ ,  $I_p(\max)$ , and  $\tau_{n1}$  for laser dyes excited by Nd-YAG laser frequencies, together with relevant photophysical properties for PLPDL systems

Laser dye <sup>a</sup>	$\lambda_{ex}$	$\lambda_{em}$	$\sigma_{01}$	$\tau_{10}$	$\sigma_{1n}$	$I_p(\max)$	$\tau_{n1}$
	[nm]		[ $10^{-17} \text{ cm}^2/\text{mol}$ ] <sup>b</sup>	[ns] <sup>c</sup>	[ $10^{-17} \text{ cm}^2/\text{mol}$ ]	[ $10^{24} \text{ photon/cm}^2 \text{ s}$ ]	[ps]
<i>p</i> -Terphenyl	266	335	16.0	0.95	143.5	12.0	31.6
<i>p</i> -Quaterphenyl	266	365	0.18	0.8	320.5	–	–
LD-390	266	386	1.00	<u>2.0</u>	140.0	–	–
	355		11.2		336.0	1.10	12.9
PBBO	266	395	1.52	1.2	31.6	–	–
	355		2.17		78.3	29.1	56.8
$\alpha$ -NPO	266	395	1.82	2.29	69.0	90.9	42.1
	355		1.06		111.0	29.8	42.0
S-420 (Silbene 420)	266	407	1.56	<u>2.0</u>	77.1	2.3	78.6
	355		17.9		501.0	9.6	81.0
DPS	266	408	0.94	1.1	211.0	–	–
	355		0.68		20.4	–	–
Bis MSB	266	418	1.83	1.3	34.0	–	–
	355		19.3		168.0	20.8	3.53
DiMe-POPOP	266	410	4.8	1.5	31.6	–	–
	355		10.3		21.4	29.7	33.8
C-450 (C-2)	266	435	2.56	<u>2.0</u>	38.6	–	–
	355		15.3		200.0	66.6	1.76
C-440 (C-120)	266	435	3.74	<u>2.0</u>	34.8	–	–
	355		11.8		26.0	62.0	35.1
C-460 (4DMC, C1)	266	445	0.1	3.2	53.6	–	–
	355		0.85		116.0	23.0	79.0
C-490 (C-151)	266	510	0.8	<u>2.0</u>	61.9	–	–
C-504 (C-314)	266	480	2.23	<u>2.0</u>	115.7	–	–
	355		0.28		41.4	–	–
C-500	266	490	4.15	<u>2.0</u>	52.1	–	–
	355		3.34		0.37	–	–
C-535 (C-7)	266	490	3.07	<u>2.0</u>	65.1	85.6	34.1
	355		0.57		34.2	–	–
C-503 <sup>F</sup> (C-307)	266	490	1.03	<u>2.0</u>	117.0	–	–
	355		1.91		59.5	–	–
C-481	266	504	3.96	<u>2.0</u>	17.5	–	–
	355		3.15		36.7	–	–
C-540 (C-6)	266	505	2.81	2.7	33.7	–	–
	355		0.54		24.5	–	–
C-515 (C-30)	266	500	1.48	<u>2.0</u>	5.0	–	–
	355		0.78		2.83	–	–
C-490 (C-151)	266	510	0.8	<u>2.0</u>	61.9	–	–
	355		3.24		172.0	32.1	38.2
Fluoresceine 548 (2,7' dichloro- fluoresceine)	266	512	3.8	4.0	14.6	–	–
	355		0.26		0.66	–	–
C-153	266	530	3.32	<u>2.0</u>	26.2	–	–
	355		0.95		77.2	37.2	49.0
Fluoresceine- disodium	266	560	3.78	6.8	6.25	–	–
	355		0.94		28.3	98.2	28.5
	532		0.46		10.3	–	–
RB	266	580	3.12	3.2	52.7	–	–
	355		1.61		88.8	74.4	3.9
	532		25.5		59.1	80.2	3.2

Table 1 (continued)

Laser dye <sup>a</sup>	$\lambda_{\text{ex}}$ [nm]	$\lambda_{\text{em}}$	$\sigma_{01}$ [ $10^{-17}$ cm <sup>2</sup> /mol] <sup>b</sup>	$\tau_{10}$ [ns] <sup>c</sup>	$\sigma_{1n}$ [ $10^{-17}$ cm <sup>2</sup> /mol]	$I_p(\text{max})$ [ $10^{24}$ photon/cm <sup>2</sup> s]	$\tau_{n1}$ [ps]
R6G	266	590	17.2	5.5	11.3	—	—
	355		3.21		138.6	75.0	3.7
	532		45.8		25.5	14.0	3.6
R640	266	600	70.9	<u>2.0</u>	48.1	—	—
	355		33.4		248.8	11.0	5.0
	532		7.20		74.9	—	—
CVP	266	625	6.14	3.5	16.0	—	—
	355		0.455		96.8	23.2	12.0
	532		9.16		1.84	—	—
DODC	355	610	1.07	1.2	4.52	—	—
DCM	266	645	4.6	1.31	20.9	—	—
	355		6.0		10.8	51.6	40.0
	532		5.3		7.6	68.8	39.6
OX 720 (OX 170)	266	650	7.63	3.0	14.25	—	—
	355		1.81		5.1	9.3	45.0
	532		3.03		5.21	—	—
LD 690	266	660	3.0	<u>2.0</u>	6.24	—	—
	355		0.5		1.94	—	—
	532		2.6		25.1	—	—
NB 690	266	670	4.66	1.7	10.7	—	—
	355		3.72		29.4	—	—
	532		1.60		1.25	—	—
OX 725 (OX 1)	266	685	12.3	1.02	8.25	—	—
	355		2.14		9.4	—	—
	532		3.05		0.4	—	—
LD 700	266	700	4.0	2.0	20.5	—	—
	532		0.24		4.72	—	—
LDS 698	266	700	3.36	<u>2.0</u>	3.51	—	—
	355		2.87		5.39	—	—
(Pyridine 1)	352		9.42		4.66	49.6	46.2
DOTC	266	725	1.91	1.2	6.2	—	—
	355		0.56		25.6	—	—
	532		0.15		6.19	—	—
HITC	266	750	1.86	1.3	3.1	—	—
	355		1.81		3.2	—	—
	532		0.46		8.0	31.1	44.4

<sup>a</sup> Exciton and/or Eastman Kodak commercial names. For correct nomenclature, where available, see Exciton "Laser Dyes" catalog. Eastman JJ-169 data service publication of laser products and [17]

RB: Rhodamine-B; R6G: Rhodamine-6G; R-640: Rhodamine-640; CVP: Cresylviolet perchlorate; OX-170: Oxazine 170; NB 690: Nile blue perchlorate

<sup>b</sup> Determined from low signal spectrophotometer readings

<sup>c</sup> Literature value where available [15–21], otherwise the value 2.0 ns was arbitrarily chosen

[15–21] for all of the laser dyes employed in the present study are summarized in Table 1. Comparison with  $\sigma_{1n}$  values for some of the dyes measured by direct  $S_1 \rightarrow S_n$  absorption flash spectroscopy [15, 22–27] and with  $\tau_{n1}$  values directly measured by picosecond techniques [15, 28] confirm the validity of the photoquenching analysis.

The importance of bleaching effects was determined by measuring the transmission of a highly attenuated laser probe beam through the irradiated pumped zone (Fig. 1b). The results shown in Fig. 15 are indicative of low transmission for intense pumping (reverse saturation) typical of excited state absorption for which  $\sigma_{1n} > \sigma_{01}$ . Moreover, if bleaching was the dominant

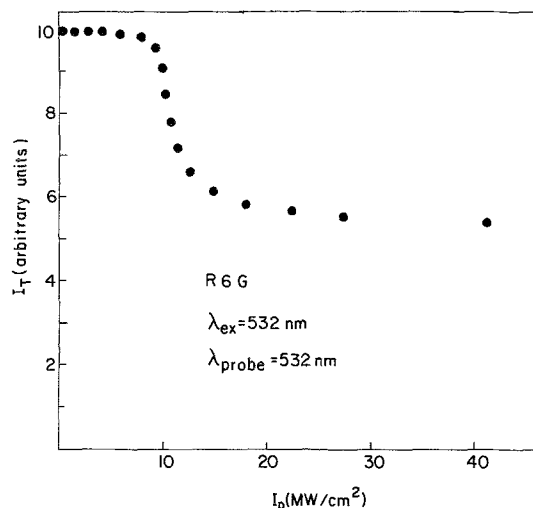


Fig. 15. Transmission curve for the R6G laser dye at 532 nm,  $I_T$  is the transmitted probe intensity (Fig. 1b) relative to the pump intensity  $I_p$

factor the slope of the  $\phi_0/\phi$  vs.  $I_p$  line would have been  $\tau_{10}\sigma_{01}$ , the fact that the cross sections obtained by this analysis differ considerably from  $\sigma_{10}$  shows that we are dealing here with a genuine photoquenching case. Since in usual laser flash spectroscopy one measures an effective absorption cross section  $\sigma_{\text{eff}} = \sigma_{1n} - \sigma_{\text{em}}$  ( $\sigma_{\text{em}}$ -stimulated emission cross section) it is not surprising that we obtain somewhat larger values for  $\sigma_{1n}$ . For obtaining values for  $\tau_{n1}$  we have to reach high pump intensities, thus limiting this method to relatively long  $\tau_{n1}$ 's for which this maximum can be reached at the pumping intensity range employed.

## Conclusions

We have demonstrated that photoquenching plays an important role in the pumping of laser dyes commonly used in PLPDL systems. Our results (Table 1) enables one to determine the optimum pumping power required for a given dye. The actual  $I_p(\text{max})$  in a PLPDL is higher than the one quoted here due to cavity losses and stimulated emission depletion of  $S_1$  population [6].

The practice of using a low-signal oscillator in an oscillator-amplifier PLPDL in commercially available systems, or the use of energy transfer for pumping dyes [8], will minimize photoquenching effects and increase the laser efficiency. In addition, we note that the photoquenching technique provides a convenient method for determining absorption cross sections for

excited states without requiring, more sophisticated, time-resolved excited-state absorption techniques. Moreover, it provides good estimate for the fluorescence lifetime of  $S_n(n \geq 2)$  state which usually requires utilization of picosecond techniques.

*Acknowledgement.* We are grateful to Miss Michal Ephrati for her help in some of the experiments. This research was supported by the Fund for the Promotion of Research of the Technion.

## References

1. S. Kimel, S. Speiser: Chem. Rev. **77**, 437 (1977) and references therein
2. S. Speiser, R. van der Werf, J. Kommandeur: Chem. Phys. **1**, 297 (1973)
3. K. Razi Naqvi, D.K. Sharma, G.J. Hoytink: Chem. Phys. Lett. **22**, 226 (1973)
4. S. Speiser: Chem. Phys. **6**, 479 (1974)  
S. Speiser, A. Bromberg: Chem. Phys. **9**, 191 (1975)
5. I. Wieder: Appl. Phys. Lett. **21**, 318 (1972)  
E. Sahar, D. Treves, I. Wieder: IEEE J. QE-**3**, 962 (1977)
6. C.D. Decker: Appl. Phys. Lett. **27**, 607 (1975)  
C.A. Moore, C.D. Decker: J. Appl. Phys. **49**, 47 (1978)
7. S. Speiser: Opt. Commun. **45**, 84 (1983)
8. S. Speiser: Appl. Phys. **19**, 165 (1979)  
S. Speiser, R. Katrarro: Opt. Commun. **27**, 287 (1978)
9. D.J. Harter, M.L. Shand, Y.B. Band: J. Appl. Phys. **56**, 865 (1984)  
W. Blau, W. Dankesreiter, A. Penzkofer: Chem. Phys. **85**, 473 (1984)
10. G. Haag, G. Marowsky: IEEE J. QE-**16**, 890 (1980)
11. G.C. Orner, M.R. Topp: Chem. Phys. Lett. **36**, 295 (1975)
12. J.C. Hindmar, R. Kugel, A. Svirnickas, J.J. Katz: Chem. Phys. Lett. **53**, 197 (1978)
13. S. Mory, D. Leupold, R. Konig: Opt. Commun. **6**, 394 (1972)
14. V.P. Klochkov, V.L. Bogdanov: Opt. Spektrosk. **39**, 666 (1975) [English transl.: Opt. Spectrosc. **39**, 374 (1975)]
15. W. Falkenstein, A. Penzkofer, W. Kaiser: Opt. Commun. **27**, 151 (1978)  
W. Blau, W. Dankesreiter, A. Penzkofer: Chem. Phys. **85**, 473 (1984)
16. I.B. Berlman: *Handbook of Fluorescence Spectra of Aromatic Molecules*, 2nd ed. (Academic, New York 1971)
17. M. Maeda, Y. Miyazoe: Jpn. J. Appl. Phys. **13**, 827 (1974)
18. E. Sahar, I. Wieder: IEEE J. QE-**10**, 612 (1974)
19. G.L. Richmond: Chem. Phys. Lett. **113**, 359 (1985)
20. J.C. Mialocq, A.W. Boyd, J. Jaraudias, J. Sutton: Chem. Phys. Lett. **37**, 236 (1976)
21. J. Fouassier, D.J. Lougnot, J. Faure: Opt. Commun. **18**, 263 (1976)
22. J. Wiedmann, A. Penzkofer: Nuovo Cimento **63 B**, 459 (1981)
23. P.R. Hammond: IEEE J. QE-**15**, 624 (1979)
24. J. Shah, R.F. Leheny: Appl. Phys. Lett. **24**, 562 (1974)
25. A. Muller, G.R. Willenbring: Ber. Bunsen Ges. Phys. Chem. **78**, 1153 (1974)
26. J.P. Fouassier, D.-J. Lougnot, F. Wieder, J. Faure: J. Photochem. **7**, 17 (1977)
27. G. Marowsky, H. Schomburg: J. Photochem. **14**, 1 (1980)
28. H. Tashiro, T. Yajima: Chem. Phys. Lett. **42**, 553 (1976)